Roles of NANOGP8 in cancer metastasis and cancer stem cell invasion during development of castration-resistant prostate cancer

Yi Sui[1#], Wei Zhang[2#], Rujian Zhu[3#], Lili Gao[4], Ting Cao[4], Chuhong Chen[3], Min Gong[3], Hongbo Zhu[5], Tao Tang[6], Bo Yu[7], Tao Yang[4]

[1]Department of Nutrition, The First Affiliated Hospital of Sun Yat-sen University, Guangzhou, China; [2]Department of Pharmacology, School of Basic Medicine, Hebei University of Chinese Medicine, Shijiazhuang, China; [3]Department of Urology, Shanghai Pudong Hospital, Fudan University Pudong Medical Center, Shanghai, China; [4]Center for Medical Research and Innovation, Shanghai Pudong Hospital, Fudan University Pudong Medical Center, Shanghai, China; [5]Department of Pathology, Shanghai Pudong Hospital, Fudan University Pudong Medical Center, Shanghai, China; [6]Department of Obstetrics and Gynaecology, Prince of Wales Hospital, The Chinese University of Hong Kong, Hong Kong SAR, China; [7]Department of General Surgery, Shanghai Pudong Hospital, Fudan University Pudong Medical Center, Shanghai, China

Contributions: (I) Conception and design: Y Sui, W Zhang, R Zhu; (II) Administrative support: B Yu, T Yang; (III) Provision of study materials or patients: B Yu, T Yang; (IV) Collection and assembly of data: L Gao, T Cao, C Chen, M Gong, H Zhu, T Tang; (V) Data analysis and interpretation: Y Sui, W Zhang, R Zhu; (VI) Manuscript writing: All authors; (VII) Final approval of manuscript: All authors.

[#]These authors contributed equally to this work.

Correspondence to: Bo Yu. Department of General Surgery, Shanghai Pudong Hospital, Fudan University Pudong Medical Center, Shanghai 201399, China. Email: yubo120@hotmail.com; Tao Yang. Center for Medical Research and Innovation, Shanghai Pudong Hospital, Fudan University Pudong Medical Center, Shanghai 201399, China. Email: taoyang@tongji.edu.cn.

Background: Prostate cancer (PCa) is one of the most common types of cancer and the emerging resistance to androgen deprivation therapy in PCa aggravates disease progression. In this study, we examined the potential pro-tumorigenic functions of NANOGP8 in prostate cancer development.

Methods: Quantitative RT-PCR confirmed higher NANOGP8 expression in androgen independent tumors, as well as a recurrent prostate tumor in patient samples. We then established a novel two-way inducible NANOGP8-short hairpin RNA experimental system, in which the NANOGP8 expression was transiently induced by adding doxycycline in the diet of NOD/SCID mice.

Results: The knockdown of NANOGP8 inhibited implanted tumor growth and the progression of castration-resistant PCa. NANOGP8-deficient PCa cells lost their cancer stem cell and gene expression programs. To further investigate the functions of NANOGP8 in PCa stem cells, real-time cell tracking was used to monitor the cell division modes and differentiation patterns of NANOGP8+ cells. The expression level of NANOGP8 markedly influenced the cell division mode of NANOGP8+ PCa cells and was strongly correlated with their pluripotency, reflected by robust telomerase activity and longer telomere length. NANOGP8 expression was also associated with the metastatic capacity of PCa cells.

Conclusions: Based on these findings, we propose that NANOGP8 could serve as an effective therapeutic target for the treatment of PCa.

Keywords: NANOGP8; prostate cancer (PCa); androgen independent tumors; cancer stem cell

Introduction

Prostate cancer (PCa) is one of the most common types of cancer and the second leading cause of cancer-associated mortality for males, particularly in Europe and the United States (1,2). Androgen signaling has been the main target for PCa treatment for more than 70 years and androgen deprivation therapy (ADT) remains the core treatment course for advanced PCa patients (3). The majority of treated patients initially respond well to ADT. However, the efficacy is often blunted by the emergence of an aggressive form of PCa termed castration-resistant prostate cancer (CRPC) (4). This may be partly related to the cellular heterogeneity of prostate tumors, in which distinct subpopulations of drug-resistant tumor cells can evade ADT and subsequently repopulate the tumor, and even grow in size (1). CRPC remains incurable and its progression is associated with the increased incidences of metastatic dissemination and patient death (5). Thus, it is imperative to understand the molecular mechanisms underlying PCa development/progression and resistance to therapy.

NANOGP8, a retrotransposed homolog of the embryonic stem cell pluripotency gene NANOG, is expressed in different types of cancers. The expression level of NANOGP8 has been positively correlated with poor survival of cancer patients (6-11). NANOGP8-expressing cancer cells possess cancer stem cell (CSC) properties and inducible expression of NANOGP8 promotes the acquisition of CSC and CRPC characteristics in PCa cells (12,13). These observations suggest that NANOGP8 might be functionally involved in the transition of PCa to the CRPC disease state.

Despite the solid evidence that NANOGP8 promotes the defined characteristics of CSCs (9,12,13) and functions as an oncogenic factor *in vitro*, it remains unresolved whether NANOGP8 has a functional role in CRPC disease progression *in vivo*. To explore this, we developed a novel experimental platform in which NANOGP8-short hairpin RNA (shRNA) induced by doxycycline (Dox) rapidly inhibited NANOGP8 expression in implanted PCa tumors. By inducing NANOGP8-shRNA at sequential stages/phases during CRPC progression, we could determine that NANOGP8 serves as an essential factor for androgen-dependent PCa tumors to acquire androgen-independence and CRPC fate.

Furthermore, to directly address whether NANOGP8 regulates PCa stem cell (PCSC) properties, we employed long-term, real-time cell tracking. The results showed that the expression level of NANOGP8 was correlated with the cell division mode of PCSCs, implying a regulatory role for NANOGP8 in the self-renewal of PCSCs.

We present the following article in accordance with the ARRIVE reporting checklist (available at http://dx.doi.org/10.21037/atm-20-1638).

Methods

Primary PCa tumor specimens and tumor processing

PCa tissues were obtained from 6 patients with primary PCa who underwent radical prostatectomy at the Department of Urology of Shanghai Pudong Hospital from December 2016 to July 2018. All tissue samples were immediately processed after surgical removal. Diagnoses and grading were histologically confirmed by two experienced pathologists according to the Gleason grading system. Tissues were fixed in 10% formalin, embedded in paraffin, and cut into 4 μm-thick sections. Sections were dewaxed and stained with hematoxylin and eosin (both from Sigma-Aldrich, St. Louis, MO, USA). The study was conducted in accordance with the Declaration of Helsinki (as revised in 2013). This study was approved by the Ethical Committee of Shanghai Pudong Hospital (No. 2015-M-01). Written consent was obtained from all patients.

Animals

Six- to eight-week-old NOD/SCID mice weighing 22 to 25 g were generated from our own breeding colonies or were purchased from the Jackson Laboratories (Bar Harbor, ME, USA). The mice were maintained in standard conditions according to the institutional guidelines. Cells (1×10^5/recipient in 0.1 mL saline) were injected subcutaneously into the left rear leg of NOD/SCID mice. All animal care and experiments were performed using approved animal protocols and the guidelines for proper conduct in animal experiments as stipulated by Shanghai Pudong Hospital (No. 2015-M-01).

Cell lines

PCa cells (LNCaP, LAPC9, and PC3) were obtained from American Type Culture Collection (ATCC, Manassas, VA, USA). LNCaP and PC3 cells were cultured in RPMI-1640 containing 8% heat-inactivated fetal bovine serum (FBS). LAPC9 cells were maintained in the NOD/SCID mice.

Xenograft procedure

LNCaP, PC3, or LAPC9 PCa cells (1×10^5/recipient) were injected into the subcutaneous area of mouse limbs. Mice were sacrificed 2 months after the initial appearance of tumors. The primary tumors were immediately harvested, weighed, and stored in −80 ℃ until use. Green fluorescent protein (GFP)-expressing primary tumors and metastases in the lungs were visualized and representative images were acquired using whole-mount epifluorescence dissecting microscopy with a model SMZ1500 instrument (Nikon, Tokyo, Japan).

Establishment of androgen-independent (AI) model

Mice were randomized into different groups (n=12/group) and were anesthetized by inhalation of 3% halothane and maintained on 1.5% halothane in 70% nitrous oxide and 30% oxygen. LNCaP, PC3, or LAPC9 PCa cells (1×10^5) were injected into the subcutaneous area of mouse limbs. After the procedure, the mice were placed at 37 ℃ and monitored in micro-isolator cages (one per cage) until they recovered from surgery. To establish androgen-dependent (AD) tumors, PCa cells were harvested and injected in Matrigel (1:1) subcutaneously into intact male NOD-SCID mice supplemented with testosterone pellets (0.8 mg/100 g body weight). To establish AI tumors, the AD tumor bearing mice were castrated at defined times according to the experimental designs, with daily intra-peritoneal injection of bicalutamide at 3 mg/100 g body weight.

Lentiviral constructs and transfection

The RRL-based lentivirus was prepared as previously described (12). In brief, G418-selected 293FT cells (1.2×10^7 cells seeded in a 15-cm dish) were transfected with the RRE (6 mg), REV (4 mg), and VSVg (4 mg) packaging plasmids, along with a lentiviral vector (6 mg) using Fugene-6 (Invitrogen, Carlsbad, CA, USA) at a 1:2.4 ratio of DNA to transfection reagent. Viral supernatants were ultra-centrifuged to produce concentrated viral stocks. Cells were plated 24 h earlier and infected with the virus prepared in parallel, at approximately 50% confluency. The 3.8-kb human NANOGP8 promoter fragment was amplified from LNCaP cell genomic DNA using the 5' primer CTC GAG CAT AGC TGC ATT GGC AAA GA and the 3' primer GGA TCC ATG AGG CAA CCA GCT CAG TC, subcloned into pCR2.1 (Invitrogen) and inserted into RRL-

PGK-GFP1 as an XhoI–BamH1 fragment before the GFP transgene to generate NANOGP8-GFP. For preparation of prostate-specific antigen-red fluorescent protein (PSA-RFP), lentivirus was produced in 293FT packaging cells and titers were determined using DsRed (Invitrogen) positivity in HT1080 cells. PCa cells were typically infected at a multiplicity of infection (MOI) of 20 and harvested at 48 to 72 h post infection.

Dox-inducible expression systems were prepared using the Nanog TRC-shRNA (Open Biosystems, Huntsville, AL, USA; oligoID: TRCN000004887) as previously described (12). LL-Nanog and TRC lentiviral packaging in 293FT packaging cells was performed using the REV, VSVg, and RRE packaging plasmids together with the individual lentivectors. The TRIPZ-nonsilencing negative control vector (cat# RHS4743), TRIPZ-Nanog68 construct (oligo ID: V2LHS_192868), and TRIPZ-Nanog22 construct (oligo ID: V2LHS_193422) were obtained from GE Dharmacon (Lafayette, CO, USA). TRIPZ constructs were packaged into lentivirus in 293T cells using the Trans-Lentiviral Packaging system (cat# TLP5913; GE Dharmacon). The pLVX-TetON-Nanog constructs harboring the NanogP8 coding region derived from LNCaP xenograft PCa cells in pCR2.1 (Invitrogen) were subcloned into the pLVXTetON expression vector (Clontech, Mountain View, CA, USA), as previously described (13). NANOG overexpression was achieved using the Lenti-X Tet-ON Advanced Inducible Expression System (Clontech) according to the manufacturer's instructions. LNCaP cells transduced with the pLVX-based lentivirus were clonally derived as previously described (13). To induce NANOGP8-shRNA in the implanted PCa cells *in vivo*, Dox was orally administered daily as a feed additive mixed with the mouse chow, at the dosage of 0.5 mg/100 mg body weight, which has been verified previously (data not shown).

Quantitative RT-PCR (qRT-PCR)

Total RNAs were isolated from cells or tumor tissues using Trizol (Invitrogen) and reverse transcribed to produce cDNA using the RNeasy Extraction Kit (Qiagen, Valencia, CA, USA) according to the manufacturer's instruction. qRT-PCR was performed in an ABI Prism 7000 Sequence Detector (Applied Biosystems, Foster City, CA, USA) using SYBR Green PCR Master Mix reagent as the detector according to the manufacturer's instructions. Primer sequences were as follows: *NANOGP8*, (forward) CGC

CCT GCC TAG AAA AGA CAT TT, (reverse) ACG AGT TTG GAT ATC TTT AGG GTT TAG AAT C; *c-Myc*, (forward) GTC AAG AGG CGA ACA CAC AAC, (reverse) TTG GAC GGA CAG GAT GTA TGC; Kruppel-like factor 5 (KLF5), (forward) CCT GGT CCA GAC AAG ATG TGA, (reverse) GAA CTG GTC TAC GAC TGA GGC; and *β-ACTIN*, (forward) CGC ACC ACT GGC ATT GTC AT, (reverse) TTC TCC TTG ATG TCA CGC AC. The expression level of each target gene was normalized to the level of β-actin using the comparative C_T method. Data were presented as the fold change in expression relative to control.

Western blot

Cell or tumor tissue lysates were collected and quantified following standard protocols. Twenty micrograms protein samples were separated by 12% sodium dodecyl sulfate-polyacrylamide gel electrophoresis, transferred to a nitrocellulose membrane, blocked for 1.5 h with Tris-buffered saline containing Tween 20 (TBST) containing 1% bovine serum albumin at room temperature, and incubated overnight with primary antibodies against Nanog (1:1,000, mouse monoclonal antibody [mAb], cat# MABD24, clone 7F7.1; Millipore, Billerica, MA, USA), androgen receptor (AR; 1:1,000, mouse mAb, cat# PP-H7507-00, clone H7507; R&D Systems, Minneapolis, MN, USA), Sox2 (1:1,000, mouse mAb, cat# MAB4423, clone 10H9.1; Millipore), FoxD3 (1:1,000, rabbit mAb, cat# 2019, clone D20A9; Cell Signaling Technology, Beverly, MA, USA), aldehyde dehydrogenase (ALDH, 1:1,000, rabbit pAb, cat# ABD12; Millipore, USA), CD44 (1:1,000, mouse mAb, cat# MA5-15462, clone 8E2F3; Invitrogen), ABCG2 (1:500, rabbit mAb, cat# ab207732, clone EPR20080; Abcam, Cambridge, MA, USA), Integrin α2β1 (1:500, mouse mAb, cat# MAB1998Z, clone BHA2.1; Millipore), Prostate-specific antigen (PSA, 1:1,000, rabbit mAb, cat# 5365S, clone D6B1; Cell Signaling Technology), Prostate-specific membrane antigen (PSMA, 1:1,000, mAb, cat# 12815S, clone D7I8E; Cell Signaling Technology), SLUG (1:1,000, rabbit mAb, cat# 9585T, clone C19G7; Cell Signaling Technology), VIMENTIN (1:1,000, mouse mAb, cat# MABT121, clone 3CB2; Millipore), Glyceraldehyde 3-phosphate dehydrogenase (GAPDH, 1:1,000, rabbit mAb, cat# 2118S, clone 14C10; Cell Signaling Technology), or β-actin (1:2,000, rabbit mAb, cat# MABT523, clone RM112; Millipore) at 4 ℃. The membranes were washed with TBST three times, then incubated with horseradish peroxidase-conjugated goat anti-rabbit or anti-mouse IgG or IgM (1:2,000; Millipore) for 1 h at room temperature, and washed again with TBST. The chemiluminescence signal was detected using ECL (Clinx Science Instruments, Shanghai, China) and developed on X-ray films. GAPDH or β-actin was used as an internal loading control.

Time-lapse imaging

Purified Nanog-GFP/PSA-RFP LNCaP cells were plated at 1×10^5 cells/well in a 6-well plate placed on the incubator stage of an AF7000 Biostation Time-Lapse system (Leica Microsystems Inc., Wetzlar, Germany), and maintained in RPMI medium supplemented with 8% FBS under at 37 ℃, 5% CO_2, and >95% humidity. GFP and RFP images were collected continuously using a 40× objective lens at a 1-h interval for 2 weeks. Representative images were captured at time points as indicated.

Lung metastasis assay

LNCaP or PC3 cells acutely purified from xenograft tumors were infected with Pcmv-GFP (Invitrogen; MOI 20, 72 h) to produce LNCaP-GFP or PC3-GFP cells. Purified GFP+ cells at the indicated numbers were injected subcutaneously into NOD/SCID male mice. All tumors were visualized in 8 weeks. Mice bearing xenograft tumors (n=12/group) were placed in the imaging box and imaged dorsally to visualize metastatic foci in the lung using the IVIS Spectrum CT In Vivo Imaging System (PerkinElmer Inc., Waltham, MA, USA).

Tissue preparation and laser capture micro-dissection (LCM)

Tissues were cryo-sectioned at 5 µm thickness on a CM3050S cryostat (Leica Microsystems Inc.), followed by standard immunostaining with anti-NANOG antibody (1:100, mouse mAb, cat# MABD24, clone 7F7.1; Millipore). The predicted NANOGP8 protein is very similar, but not identical, to the embryonic stem cell-specific NANOG1 protein. Hence, most anti-NANOG1 antibodies tested react well with the NANOGP8 protein in PCa cells. Consequently, the NANOG1/NANOGP8 proteins are often simply termed NANOG. Sections were further incubated with fluorescein isothiocyanate (FITC)-conjugated goat anti-mouse IgG (1:100; Millipore). Rinsed sections were counter-stained with 10 µg/mL 4',

6-diamidino-2-phenylindole (DAPI; Sigma-Aldrich). Normal IgG was used as a negative control. NANOG^{+} cells (green) were visualized by the PixCell II LCM system (Arcturus Engineering, Mountain View, CA, USA). After micro-dissection with a spot size of 7.5 μm and a pulse duration of 1.5 ms (power 50 mW), the dissected region as indicated was collected in a 0.5-ml micro-centrifuge tube and used for western blotting analysis.

Flow-fluorescence in situ hybridization (flow-FISH)

Flow-FISH was conducted to measure the telomere length of cells. Calibration of the flow cytometer, cell fixation, staining protocol, and normalization were conducted using mouse lymphoma cells with known telomere length. Purified cells (5×10^5) or mouse lymphoma cells (control) were washed in hybridization buffer and resuspended in hybridization solution containing formamide and 0.3 μg/mL fluorescein isothiocyanate (FITC)-conjugated pentose nucleic acid (PNA) probe. Control samples were incubated in hybridization solution in the absence of PNA probe. Lymphoma cells were distinguished from cell derivatives by immunostaining with CD45 antibody (Millipore). DNA content was quantified using propidium iodide staining. Cells were gated at G0/G1 based on DNA content, and the fluorescence intensity of telomeres was calculated as previously described (14). Detections were conducted on the FACSCanto flow cytometer (Becton Dickinson, Franklin Lakes, NJ, USA).

Cell invasion assay

A cell invasion assay was performed using 24-well Biocoat Matrigel invasion chambers with an 8.0-μm pore size (BD Bioscience Discovery Labware, Sedford, MA, USA) according to the manufacturer's instructions. Briefly, 5×10^4 ALDH^{+}CD44^{+}α2β1^{+} cells were loaded into the upper chamber that was coated with Matrigel (100 μg/mL; BD Biosciences) diluted 1:20 in Dulbecco's modified Eagle's medium (DMEM) filled with 500 μL DMEM containing 0.1% FBS. To induce cell invasion, 600 μL 10% FBS-containing DMEM was loaded into the lower chamber. After incubation overnight, non-invading cells remaining in the upper chamber were removed with a cotton swab. The invading cells adhering to the lower surface were fixed and stained using crystal violet. The stained cells were counted in 10 randomly selected fields under a model IX71 inverted light microscope (Olympus, Tokyo, Japan).

Statistical analyses

Statistical analyses were performed using SPSS 23.0 software (SPSS Inc., Chicago, IL, USA). Unless stated otherwise, normally distributed data are presented as the mean ± standard deviation of at least three independent experiments. Multiple groups were compared by ANOVA followed by post hoc analysis (S-N-K test). A two-tailed P value < 0.05 was considered statistically significant.

Results

NANOGP8 expression level is associated with AI and PCa recurrence

In AD and AI implanted tumors caused PCa cells, qRT-PCR revealed a significantly higher (approximately 5-fold) expression level of NANOGP8 mRNA in the implanted tumors of the AI group compared to AD group (*Figure 1A*). High expression of NANOG protein has been linked to the occurrence, development, recurrence, and metastasis of breast cancer (15,16).

To examine if the NANOGP8 expression level was correlated with the recurrence of PCa, we compared the paired PCa tissue samples obtained before treatment (pre-therapy) and the recurrent tumors. Tissue microarray and histological analysis revealed that the recurrent PCa tumors appeared as solid masses (*Figure 1*) and lost the pseudo-glandular "cavity-like" structures normally observed in pre-therapy PCa samples (*Figure 1B,C*). Moreover, western blot demonstrated an elevated expression level of NANOGP8 protein in recurrent PCa tumor samples compared to the paired samples from pre-therapy (*Figure 1D*). Based on these results, we hypothesized that there is a link between NANOGP8 expression and the differential phenotypes or characteristics of PCa, such as AD and the propensity for tumor recurrence.

Knockdown of NANOGP8 inhibits growth and progression of implanted prostate tumors during CRPC progression

NANOGP8 is an essential factor in the production of CRPC (9,12,13). However, the role of NANOGP8 in regulating the dynamic progression of AD implanted tumor to AI and CRPC remains unresolved, as most studies manipulated NANOGP8 level before implanting PCa tumors, which only reflects a "static" view of NANOGP8 function in the formation of CRPC.

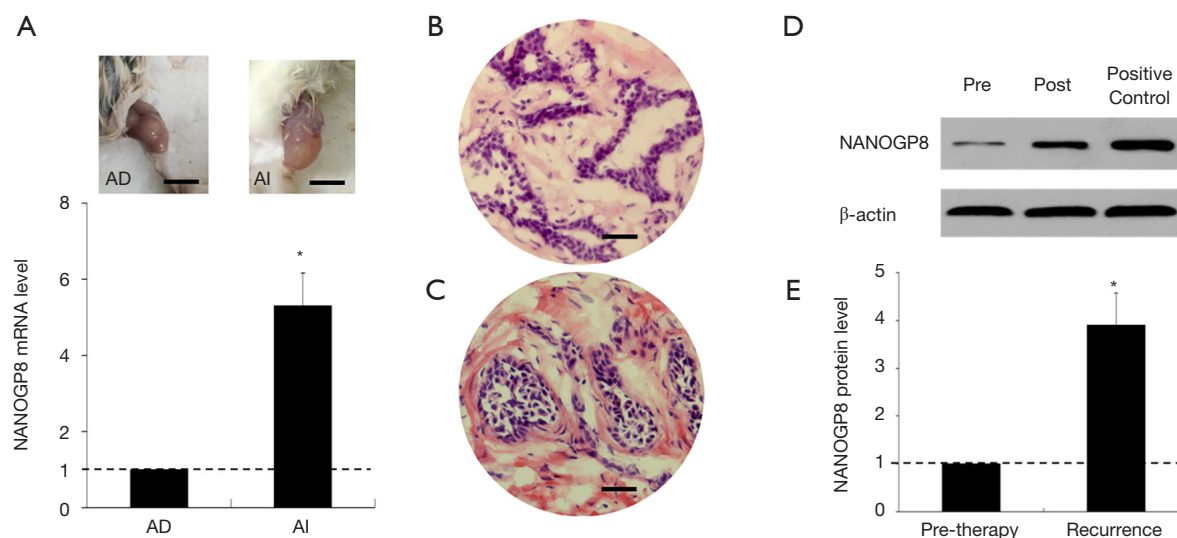To circumvent this clinically significant issue and

Page 6 of 15

Sui et al. NANOGP8 in cancer metastasis and cancer stem cell invasion

Figure 1 NANOGP8 expression levels in implanted tumors and human prostate cancers. (A) qRT-PCR analysis of implanted human tumors showed that the expression level of NANOGP8 mRNA in the androgen-independent (AI) group was significantly higher than that of androgen-dependent (AD) group (scale bar: 10 mm). (B,C) Comparative analysis of tissue microarray showed the morphology of tumor before treatment (B, scale bar: 30 μm) and of recurrent tumor after treatment (C, scale bar: 30 μm) [Hematoxylin-Eosin (HE) staining]. (D,E) Western blot analysis showed NANOGP8 protein expression levels (D). Compared to "before treatment", the expression level of NANOGP8 protein after prostate cancer recurrence was significantly higher (E). Positive control is human leukemia Jurkat cell line.

to improve our understanding of the *in vivo* role of NANOGP8 in CRPC development, we established a novel two-way reversible Dox-inducible NANOGP8-shRNA system (*Figure 2A*), which provides a transient and reversible knockdown for NANOGP8 in PCa cells. Similar to the Dox-inducible NANOG overexpression system, LNCaP, LAPC9 and PC3 cell lines (all from AD implanted tumors), were transduced with the Tet-ptTS-Neo lentiviral vector and used to establish stable cell clones. These cell clones also contained a self-inactivating retroviral expression vector designed to express NANOGP8 shRNA only upon Dox induction. As expected, the expression level of NANOGP8 mRNA was significantly decreased in the presence of Dox, as confirmed by quantitative RT-PCR in all cell clones (*Figure 2B*).

Next, we implanted LNCaP/dox-NANOGP8 shRNA and LAPC9/dox-NANOGP8 shRNA cell lines onto male mice host and harvested these tumors at different stages during the prostate tumor progression (AD, AI, and CRPC, see *Figure 3A*). After 10 weeks of implantation (Stage 1), AD tumors were analyzed by western blotting. As expected, the NANOGP8 protein level was reduced in the presence of Dox-augmented diet, compared to untreated control.

Meanwhile, we observed the expression level of AR and PSA were up-regulated, while CD44 expression was decreased. When the implanted tumors were transformed from AD into AI tumors, following the castration treatment (removal of testis and intra-peritoneal injection of bicalutamide) for 12 weeks (Stage 2), we found that Dox treatment remained effective to lower NANOGP8 protein level and observed the same trend of changes in the expression level of AR, PSA, and CD44. Lastly, when the AI tumor developed into CRPC with 12 weeks of castration treatment (Stage 3), the protein level of NANOGP8 still could be reduced by consumption of the Dox containing diet, which resulted in lower expression of CD44 and higher expression of AR and PSA (*Figure 3B,C*).

Given that NANOGP8 level was correlated with AI phenotypes and recurrent prostate tumors, the Dox-inducible NANOGP8 shRNA system was exploited to examine the effects of NANOGP8 knockdown on implanted tumor growth. With the consumption of the Dox diet, the implanted LAPC9 tumors exhibited significant growth retardation in all stages tested (Stage 1 to 3; *Figure 4*), which was consistent with its role for the tumor regeneration in LNCaP cells (13).
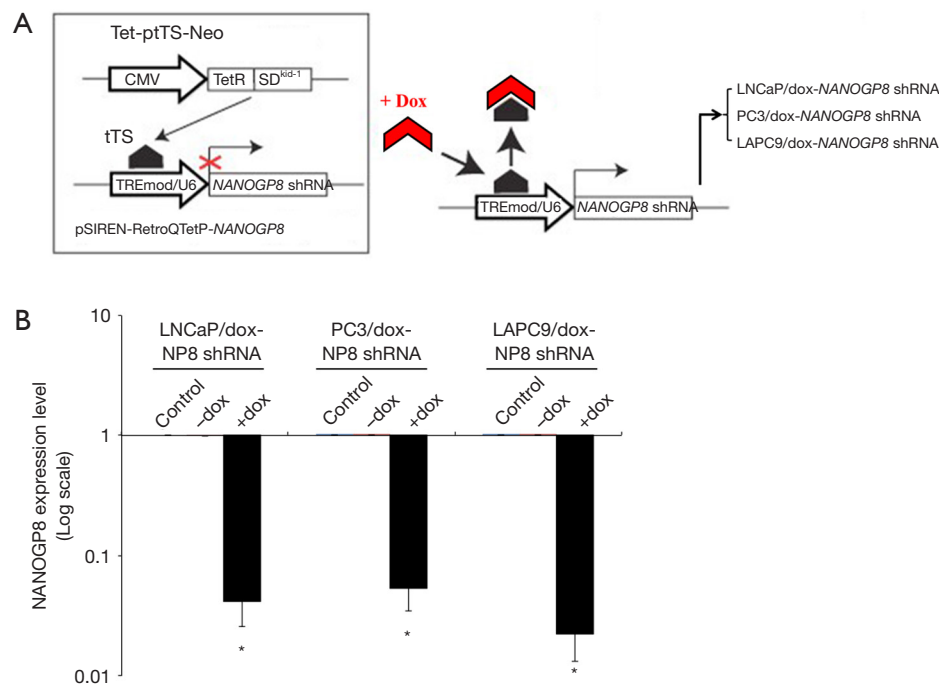
Figure 2 Doxycycline-inducible knockdown system for NANOGP8. (A) Schematic diagram of doxycycline-inducible NANOGP8 knockdown system; (B) In prostate cancer cell culture, qRT-PCR experiments confirmed that the expression level of NANOGP8 mRNA in LNCaP-, PC3-, and LAPC9-derived doxycycline-inducible NANOGP8 knockdown system was significantly decreased respectively when doxycycline (dox) was present. *P<0.05 *vs.* –dox.

Knockdown of NANOGP8 affects the expression of CSC genes

The dependence of CD44 expression on NANOGP8 level as well as the role of NANOGP8 in AI and CRPC tumor growth/regeneration suggested the involvement of NANOGP8 in the regulation of PCSCs (17). LCM of implanted CRPC tumors induced via castration (*Figure 2*) revealed that NANOGP8-expressing tumor cells/areas co-expressed the known CSC markers ALDH, integrin α2β1, and CD44, with only minimal PSA expression (17-19) (*Figure 5*), which was consistent with previous observations suggesting the ability of NANOGP8 to promote stemness in PCa cells (13). Furthermore, mimicking the castration environment by adding charcoal dextran-stripped serum and bicalutamide to the culture medium of LNCaP cells resulted in the increased expression of NANOGP8 and other "stemness" genes, including SOX2 and FOXD3 (*Figure 6*). Differentiation markers, such as AR and PSA, were reduced (*Figure 6*). The collective findings demonstrated that castration promotes PCSC characteristics, among which NANOGP8 is a pivotal regulator.

Knockdown of NANOGP8 affects cell division modes and metastatic capacity of PCSCs

To further understand the role of NANOGP8 in PCSCs, real-time cell tracking by time-lapse video microscopy was used to monitor the cell division modes and differentiation patterns of NANOGP8+ cells. After sorting out NANOGP8-GFP+ cells from LNCaP-derived implanted tumors, PSA-RFP lentiviral vector was transfected and used as the differentiation marker (*Figure 7A*). Two weeks of monitoring with approximately 200 microscopy data points revealed that within 72 h under normal culture conditions, the parental NANOGP8-GFP+ cells could produce 23.2%±4.6% GFP+ daughter cells. Some of these cells would start to express RFP indicative of PSA expression, either by asymmetric cell division, which took 18.6±5.8 h, or symmetric differentiation (*Figure 7B*). On the other hand, if endogenous NANOGP8 was inhibited by shRNA lentiviral vector after 12 h of culture, the NANOGP8-GFP+ population was significantly diminished and the cell division pattern was dominated by symmetric differentiation, which resulted in 85.2%±12.1% of daughter cells that expressed
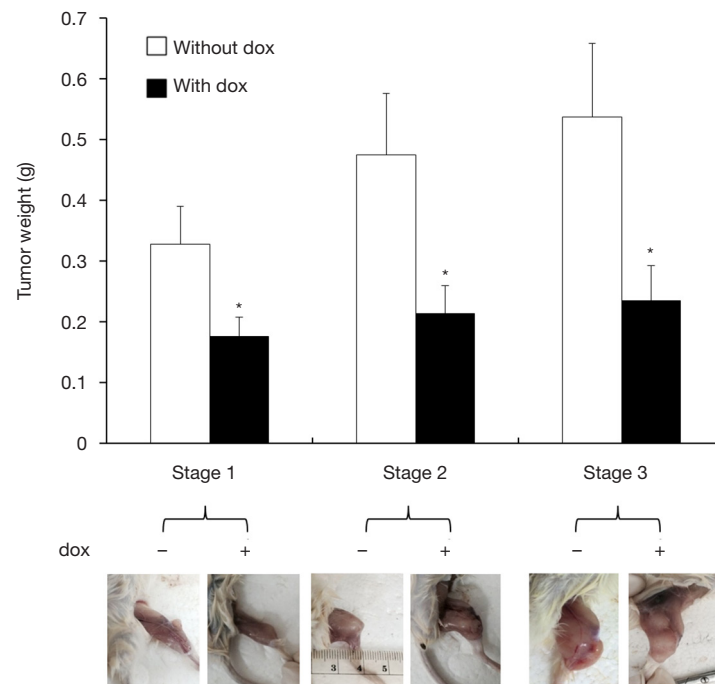
Figure 3 Knockdown of NANOGP8 changed cell state of implanted prostate tumors during castration-resistant prostate cancer progression. (A) Schematic diagram of experimental design; (B) Western blot analysis for tumors derived from LNCaP/dox-NanogP8 shRNA with or without doxycycline (dox) administration at the end of time courses as indicated. AD refers to androgen dependent tumors at 10 weeks post LNCaP (wild-type) cell implantation; while AI refers to androgen independent tumors, derived from AD tumors, after 12-week castration treatment. (C) Quantitation of (B). Band intensities were quantified by using Image Lab Software (Bio-Rad, Hercules, CA, USA) and the protein expression level was normalized to the level of β-actin. Data in (B) were presented in logarithm scale as the fold change in expression relative to wild type LNCaP cell-derived AD tumors (n=6). *P<0.05 *vs.* Stage 1 (-dox); #P<0.05 *vs.* Stage 2 (-dox); ΔP<0.05 *vs.* Stage 3 (-dox).

RFP (*Figure 7C*). If bicalutamide (20 μM) was added to the culture medium at the beginning of real-time tracking to mimic the castration environment *in vivo*, the NANOGP8-GFP⁺ cells were stimulated to engage in continuous symmetric cell division, resulting in colonies strongly dominated by GFP⁺ cells (89.2%±8.5%) (*Figure 7D*).

Finally, the metastatic tendency of CRPCs makes this kind of cancer particularly difficult to treat. Thus, we investigated the involvement of NANOGP8 in prostate cancer metastasis. Orthotopic implantation of LNCaP and PC3 cells that were transfected with GFP and expressed dox-NANOGP8 shRNA (LNCaP or PC3/dox-NANOGP8 shRNA line) often resulted in metastasis and migration of the cells to the lungs. When Dox was administrated, metastasis of GFP⁺ cells was significantly decreased in the lungs of tumor bearing mice at all stages tested (stage 1-3) (*Figure 8*). Consistently, the castration treatment on LNCaP cells *in vitro* led to increased expression of the epithelial-

mesenchymal transition markers SLUG and VIMENTIN (*Figure 6*), which were likely associated with the expression of NANOGP8.

NANOGP8⁺ cells possess more robust telomerase activity and longer telomere length

As shown above, some pluripotency markers, including ALDH, CD44, and α2β1, were highly expressed in PCSCs (*Figure 5*). In LAPC9-derived implanted tumors, after sorting cells according to the expression level of these three genes, we observed robust NANOGP8 expression (GFP⁺) using NANOGP8-GFP as a reporter in ALDH⁺ CD44⁺ α2β1⁺ cells, while ALDH⁻ CD44⁻ α2β1⁻ cells remained negative for NANOGP8 expression (GFP⁻) (*Figure 9A*). These results supported the notion that NANOGP8⁺ cells express high levels of pluripotency markers, representing at least in part the subpopulation of

Figure 4 Knockdown of NANOGP8 inhibit tumor growth. The weight of LAPC9-derived tumor was measured at 3 different time points (Stage 1 to 3) after administration of doxycycline (dox). *P<0.05 *vs.* without dox.

Figure 5 Cancer stem cell markers are co-expressed with NANOGP8 in CRPC (castration-resistant prostate cancer) tumors. Surgery and chemical castration induced mouse implanted tumors to form CRPC. (A-C) Immunofluorescence staining showed that NANOG antibody (recognizing NANOGP8 in tumor samples) could specifically bind to Region 1 in the pathological section of the implanted tumor; Using laser micro-dissection to isolate Region 1 and Region 2 as indicated in the section. (D) Immunoblotting indicated that the cellular phenotype of Region 1 (NANOGP8+) is PSA⁻ PSMA⁻/ALDH⁺ CD44⁺ α2β1⁺ ABCG2⁺. Scale bars, 25 µm.
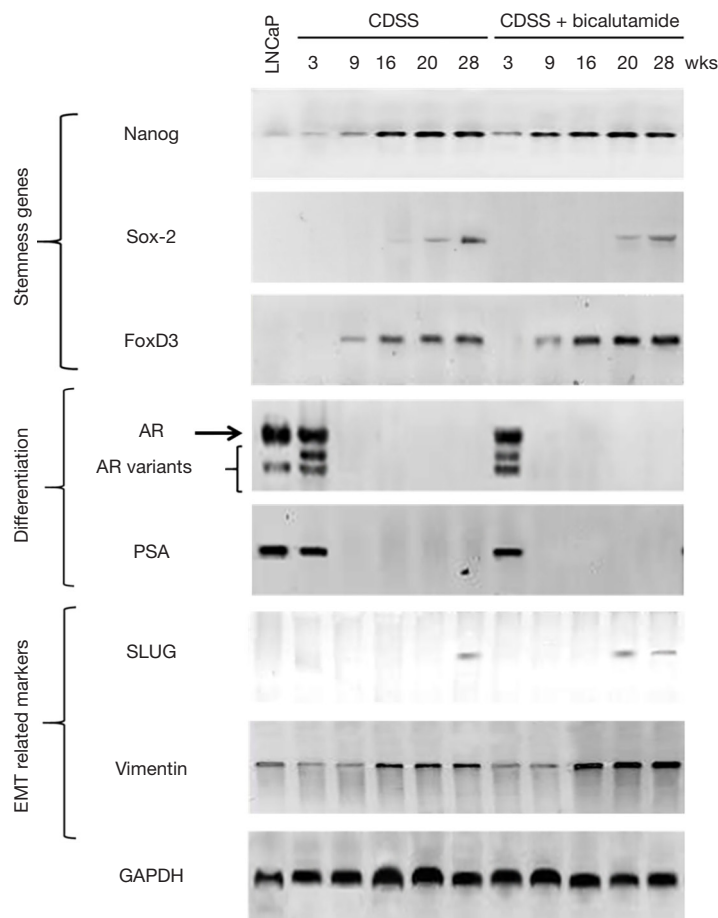
Figure 6 Dynamic changes of cellular phenotype and NANOGP8 expression during *in vitro* culture of induced CRPC cell model. (A) Chemically castration (charcoal dextran-stripped serum (CDSS) and CDSS+bicalutamide) induced the progressive reduction of epithelial cell markers, AR and PSA, during the transformation of LNCaP cells into a CRPC cell model, while gradually increased the expression of mesenchymal markers, such as SLUG, VIMENTIN and stemness related genes (NANOG, SOX-2, FOXD3).

primitive PCSCs.

To further demonstrate the pronounced pluripotency of NANOGP8+ cells (ALDH+ CD44+ α2β1+ and GFP+), we examined the telomerase activity and telomere length of these cells. Both aspects correlate with stemness (20). Using qPCR, we observed significantly stronger telomerase activity in NANOGP8+ cells derived from xenograft tumors (Passage 0), compared to NANOGP8− cells, in the ALDH− CD44− α2β1− or PSA+ subgroups (*Figure 9B*). Similar results were also obtained in Passage 5 (*Figure 9B*). Next, we examined telomere length quantitatively by FISH in combination with flow-FISH. NANOGP8+ cells displayed longer telomeres compared to all other populations, including unsorted cells, ALDH− CD44− α2β1−, or PSA+

subpopulations (*Figure 9C*). These results reinforced the conclusion that NANOGP8 is a stemness/pluripotency marker for PCSCs.

c-Myc and KLF5 act as downstream effectors for NANOGP8

To explore the downstream targets of NANOGP8, we examined c-Myc and KLF5, since both were suggested as downstream effectors of NANOGP8, based on a previous report (21) as well as our transcriptome analysis (data not shown). To further validate the regulatory relationship between NANOGP8 and c-Myc as well as KLF5, we manipulated the expression of NANOGP8 in PC3 PCa cell
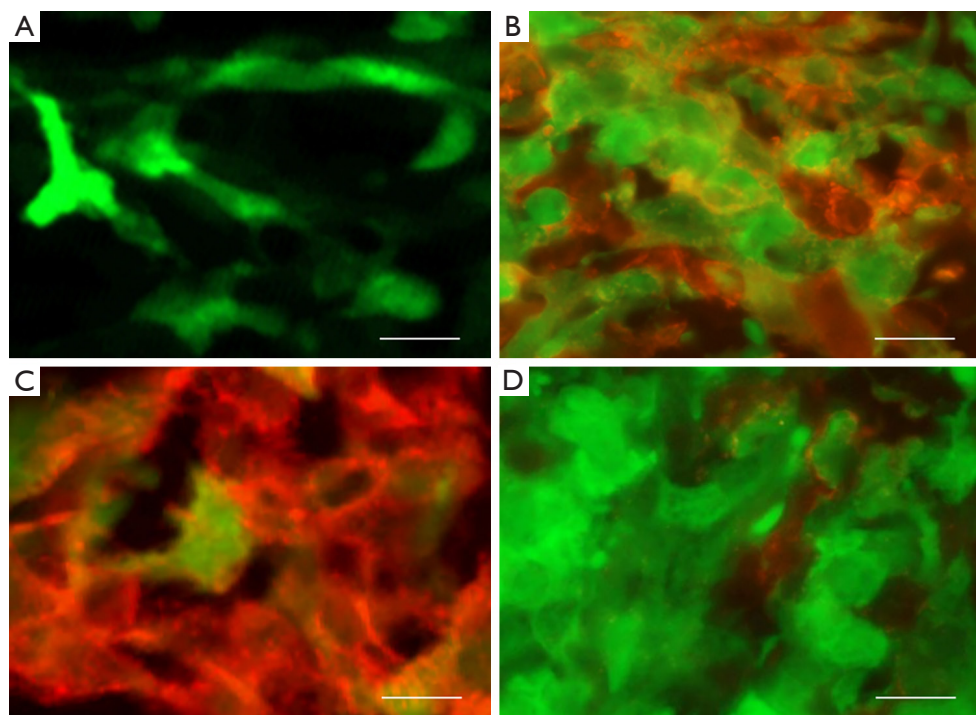
Figure 7 Real-time monitoring of cell division and differentiation patterns of NANOGP8-GFP⁺ cells. (A) Parental NANOGP8-GFP⁺ cells. (B) Under normal culture conditions, NanogP8-GFP⁺ cells produced GFP⁻ cells by asymmetric division and express PSA-RFP. (C) When endogenous NANOGP8 was knocked down by lentiviral shRNA, its cell division mode would become dominant with symmetric differentiation. (D) Under *in vitro* castration environment by adding androgen antagonists, NANOGP8-GFP⁺ cells continued to undergo symmetric division, which would lead to colonies that were dominated by GFP⁺ cells. Scale bar, 5 µm.
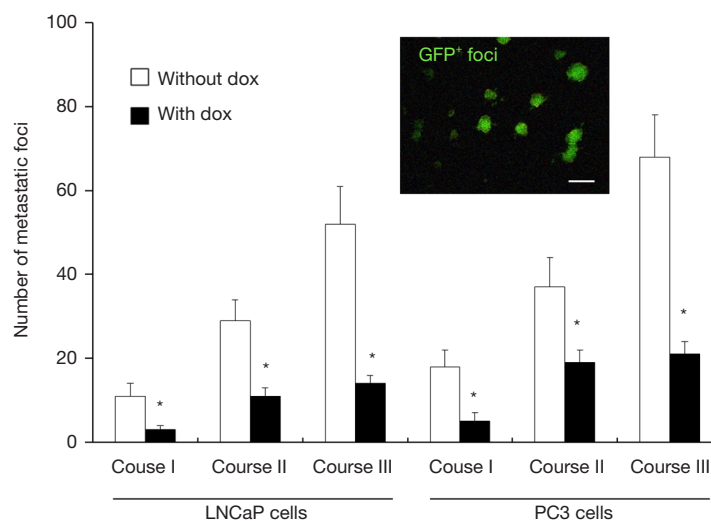
Figure 8 Knockdown of NANOGP8 decrease the metastatic capacity of prostate tumors. LNCaP-GFP and PC3-GFP cells were implanted into mouse prostate, and the number of GFP⁺ metastases in the lungs of tumor-bearing mice was detected in Stage 1, Stage 2 and Stage 3, respectively. *P<0.05 *vs.* without dox. Scale bar: 80 µm.

Page 12 of 15

Sui et al. NANOGP8 in cancer metastasis and cancer stem cell invasion
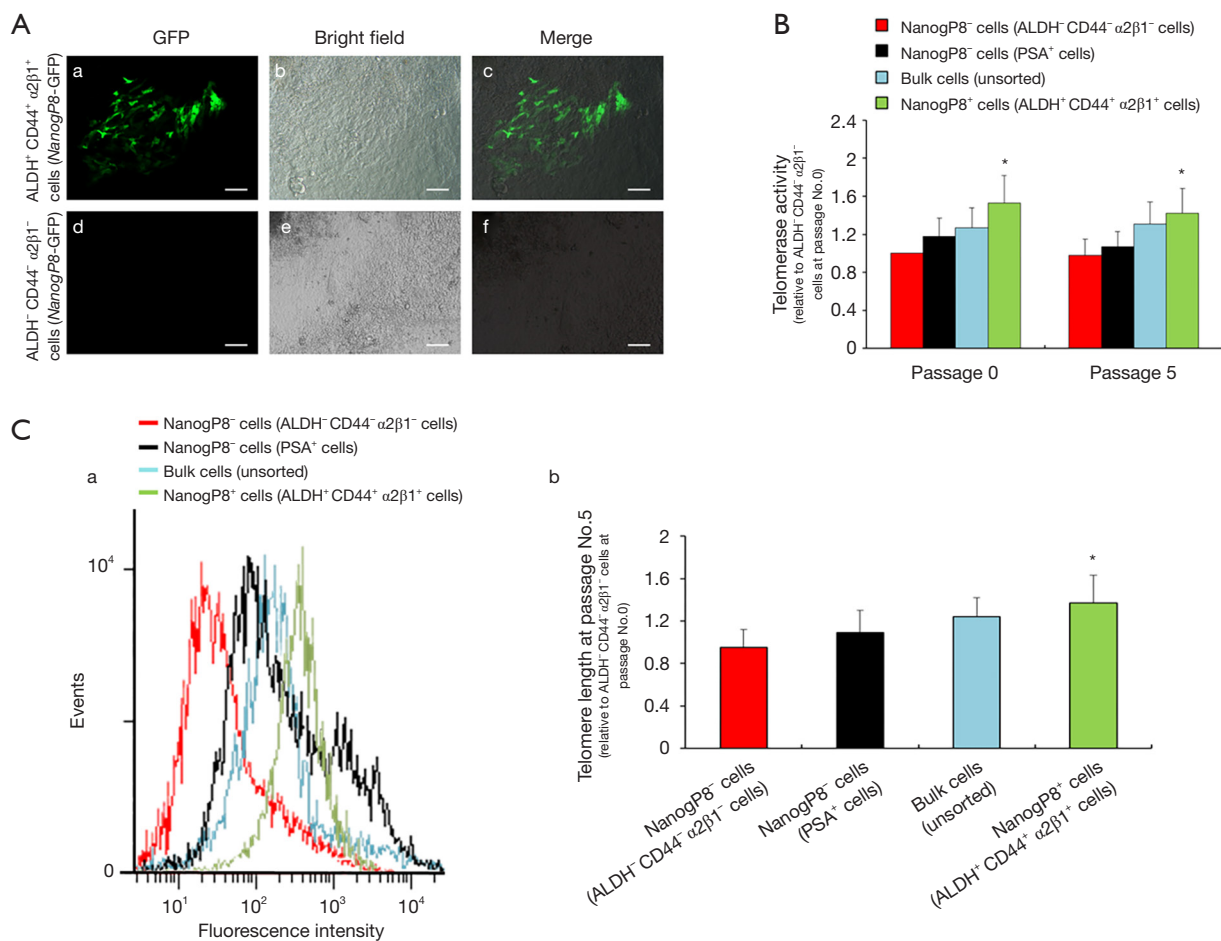
Figure 9 NANOGP8+ cells possess more robust telomerase activity and longer telomere length. (A) The LAPC9-derived tumor was digested into discrete cells, which were then sorted according to the expression status of ALDH, CD44 and integrin α2β1. NANOGP8-GFP was transfected as expression reporter for NANOGP8. In the bulk culture, ALDH+ CD44+ α2β1+ cells after 2 days *in vitro* culture, exhibited a "salt and pepper" pattern of GFP expression (a-c), whereas ALDH– CD44– α2β1– cells consistently showed no (or very low) expression of GFP (representing negligible expression of NANOGP8) (d-f). Scale bars, 30 μm. (B) The telomerase activity was evaluated by quantitative PCR for cell populations as indicated. (C-a) Quantitative measurements of telomere length were conducted by flow-fluorescence in situ hybridization (flow-FISH), and the results indicated that the length of telomere is longer in ALDH+ CD44+ α2β1+ cells. (C-b) Fold change in telomere length relative to ALDH– CD44– α2β1– cells at Passage 0 (i.e., directly derived from xenograft tumor in mice). *P<0.05.

lines by Dox-inducible shRNA (knockdown) or NANOGP8 cDNA (overexpression). The expressions of both c-Myc and KLF5 were changed concomitantly with the level of NANOGP8 expression. Knockdown of c-Myc resulted in the down-regulation of KLF5, but not NANOGP8. The findings indicated that c-Myc and KLF5 were downstream of NANOGP8 (*Figure 10A,B*).

In addition, since as NANOGP8 promoted PCa cell migration (*Figure 8*), we examined if c-Myc and KLF5 regulated cell migration as well by *in vitro* cell invasion assay. As predicted, knockdown of NANOGP8 reduced the number of cells that invaded through Matrigel. Simultaneous knockdown of c-Myc and KLF5 further reduced cell invasion. These results suggested that c-Myc and KLF5 are the downstream effectors for NANOGP8 (*Figure 10C*).
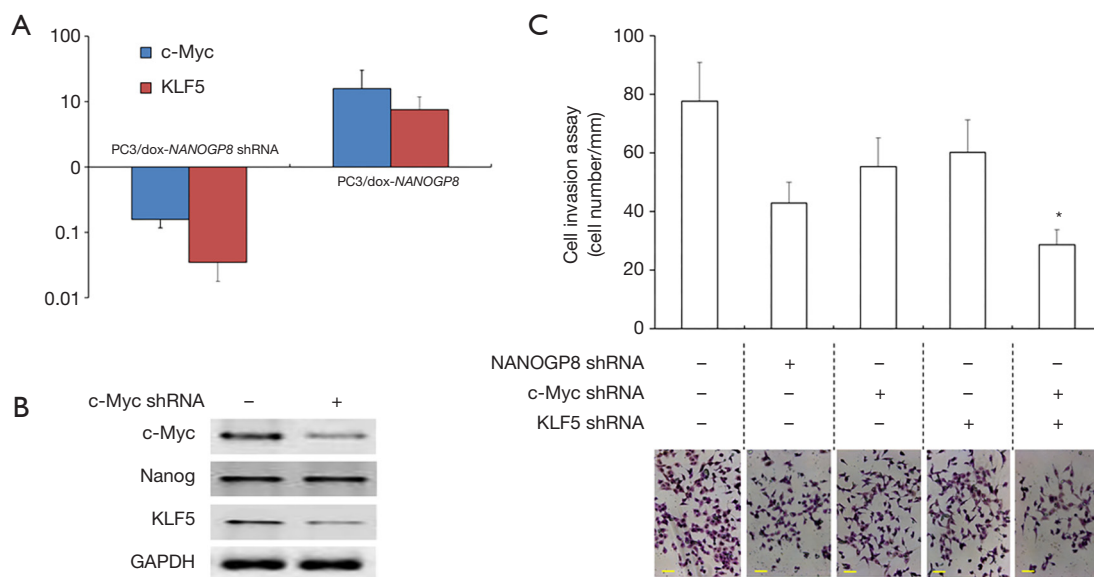
Figure 10 c-Myc and KLF5 are regulated by NANOGP8 expression. (A) Using dox-inducible expression system, when knocking-down NANOGP8, expression levels of c-Myc and KLF5 were also significantly reduced. Conversely, NANOGP8 overexpression with dox led to the up-regulation of c-Myc and KLF5. (B) Knockdown c-Myc by short hairpin RNA (shRNA) only affected KLF5 expression but not NANOGP8. (C) Matrigel cell invasion assay showed that knocking-down NANOGP8, c-Myc and KLF5 all reduced the ability of cells undergoing invasion (shown as number of cells migrating through matrigel). Co-expression of c-Myc and KLF5 shRNA showed synergistic effects and further reduced cell invasion events, when compared to c-Myc shRNA alone or KLF5 shRNA alone. Representative images of invading cells were shown at bottom panel. Representative images in (C): crystal violet staining. Scale bars, 400 µm. *, P<0.05 *vs*. c-Myc shRNA alone or KLF5 shRNA alone.

Discussion

Endogenous NANOGP8 is essential for growth of castration-resistant PCa

We used a novel experimental platform that allowed Dox-induced shRNA knockdown of NANOGP8 in PCa cell lines and xenografts. The results strongly supported the notion that NANOGP8 plays a key role in the regulation of prostate tumor development, especially during the acquisition of AI and transformation to CRPC (*Figures 2* and *3*). The findings were consistent with previous studies from several other groups (12,13,15,21,22). Together with the positive correlation between the NANOGP8 expression level and AI phenotype (*Figure 1*) as well as castration treatment (*Figure 6*), we believe our result validate the pivotal role of NANOGP8 in dynamic transition of AD to AI tumors and subsequent development of CRPC.

The underlying mechanisms that might be responsible for NANOGP8-conferred AI phenotypes and castration resistance are likely linked to the AR signaling status in the PCa cells. Indeed, the lower expression level of AR evident in PCSCs might explain their intrinsic independence on AR signaling (17,23,24). Consistent with the reciprocal nuclear expression between AR and NANOGP8 (12), we also demonstrated that *in vivo* knockdown of NANOGP8 in implanted PCa cells resulted in higher expression level of AR (*Figure 3*). The AR signaling axis plays a critical role in the development, function, and homeostasis of the prostate as well as in prostate carcinogenesis and progression to an AI disease state (25). Thus, further understanding of the critical events and complexities of AR signaling during the progression to CRPC is essential for the successful development of efficacious therapies.

NANOGP8 may maintain pluripotency of PCSCs by regulating their cell division modes

Long-term, real-time cell tracking with time-lapse microscopy revealed that NANOGP8 governs the cell division modes of PCa cells, including symmetric stem cell renewal (dividing symmetrically to generate two stem cells), asymmetric stem cell renewal (generating one stem cell and another differentiated daughter cell), and symmetric

Page 14 of 15

Sui et al. NANOGP8 in cancer metastasis and cancer stem cell invasion

stem cell differentiation (dividing symmetrically to generate two differentiated daughter cells). The three division modes depended on the expression level of NANOGP8 (*Figure 8*). NANOG has been demonstrated to be essential to maintain the self-renewal of embryonic stem cells. Thus, it is reasonable to hypothesize that CSC-expressed NANOGP8 will engage similar, if not the same, downstream transcriptional responses, which dictate the stem cell properties and behaviors. Consistent with this hypothesis, we found a strong correlation between NANOGP8 expression level and the stemness of PCa cells, reflected by robust telomerase activity and longer telomere length (*Figure 9*).

NANOGP8-regulated gene expression programs correlate with patient transcriptomes and prognosis/survival, including AR/FoxA1 signaling axis and molecules involved in castration resistance, such as Bcl-2, IGFBP-5, and CXCR4 (13,21). The present transcriptome analysis also identified c-Myc and KLF5 as downstream effectors for NANOGP8, consistent with previous studies (13,21). However, given that NANOGP8 influences the cell division mode of CSCs, the findings strongly suggest that NANOGP8 might regulate the cell polarity complex or segregating determinants, such as Numb (26). We are currently investigating these possibilities.

NANOGP8 as a therapeutic target for PCa treatment

Recurrence of PCa after ADT treatment usually involves tumor cells that are prone to develop castration resistance and progress to the CRPC disease state. This is a devastating condition and currently incurable. The data presented here indicate that NANOGP8 regulates CRPC growth and, importantly, reduces NANOGP8 expression to effectively halt tumor growth during the progression of CRPC at any stage (*Figure 3*). The findings implicate NANOGP8 as an excellent therapeutic target in the treatment of PCa. Further studies to elucidate the underlying mechanism are underway. In addition, previously identified downstream targets or interacting pathways (13,21) may be potentially used in combination with NANOGP8 to treat CRPC, which would expand the therapeutic arsenal for PCa.

Acknowledgments

Footnote

References

1. Siegel RL, Miller KD, Jemal A. Cancer statistics, 2016. CA Cancer J Clin 2016;66:7-30.
2. Ferlay J, Steliarova-Foucher E, Lortet-Tieulent J, et al. Cancer incidence and mortality patterns in Europe: estimates for 40 countries in 2012. Eur J Cancer 2013;49:1374-403.
3. Sternberg CN. Systemic chemotherapy and new experimental approaches in the treatment of metastatic prostate cancer. Ann Oncol 2008;19:vii91-5.
4. Scher HI, Halabi S, Tannock I, et al. Design and end points of clinical trials for patients with progressive prostate cancer and castrate levels of testosterone: recommendations of the Prostate Cancer Clinical Trials Working Group. J Clin Oncol 2008;26:1148-59.
5. Logothetis CJ, Lin SH. Osteoblasts in prostate cancer metastasis to bone. Nat Rev Cancer 2005;5:21-8.
6. Zhang J, Wang X, Li M, et al. NANOGP8 is a retrogene expressed in cancers. The FEBS J 2006;273:1723-30.
7. Uchino K, Hirano G, Hirahashi M et al. Human Nanog pseudogene8 promotes the proliferation of gastrointestinal cancer cells. Exp Cell Res 2012;318:1799-807.
8. Palla AR, Piazzolla D, Abad M et al. Reprogramming activity of NANOGP8, a NANOG family member widely expressed in cancer. Oncogene 2014;33:2513-19.
9. Zhang K, Fowler M, Glass J, et al. Activated 5-flanking region of NANOGP8 in a self-renewal environment is associated with increased sphere formation and tumor growth of prostate cancer cells. Prostate 2014;74:381-94.
10. Ishiguro T, Sato A, Ohata H, et al. Differential expression of nanog1 and nanogp8 in colon cancer cells. Biochem Biophys Res Commun 2012;418:199-204.
11. Zhang J, Wang X, Chen B, et al. The human pluripotency gene NANOG/NANOGP8 is expressed in gastric cancer and associated with tumor development. Oncol Lett 2010;1:457-463.
12. Jeter CR, Badeaux M, Choy G, et al. Functional evidence that the self-renewal gene NANOG regulates human tumor development. Stem Cells 2009;27:993-1005.
13. Jeter CR, Liu B, Liu X, et al. NANOG promotes cancer stem cell characteristics and prostate cancer resistance to androgen deprivation. Oncogene 2011;30:3833-45.
14. Baerlocher GM, Vulto I, de Jong G, et al. Flow cytometry and FISH to measure the average length of telomeres (flow FISH). Nat Protoc 2006;1:2365-76.
15. Paranjape AN, Balaji SA, Mandal T, et al. Bmi1 regulates self-renewal and epithelial to mesenchymal transition in breast cancer cells through Nanog. BMC Cancer 2014;14:785.
16. Lu X, Mazur SJ, Lin T, et al. The pluripotency factor nanog promotes breast cancer tumorigenesis and metastasis. Oncogene 2014; 33:2655-64.
17. Patrawala L, Calhoun T, Schneider-Broussard R, et al. Highly purified CD44+ prostate cancer cells from xenograft human tumors are enriched in tumorigenic and metastatic progenitor cells. Oncogene 2006;25:1696-708.
18. Patrawala L, Calhoun-Davis T, Schneider-Broussard R, et al. Hierarchical organization of prostate cancer cells in xenograft tumors: the CD44+alpha2beta1+ cell population is enriched in tumor-initiating cells. Cancer Res 2007;67:6796-805.
19. Qin J, Liu X, Laffin B, et al. The PSA(–/lo) prostate cancer cell population harbors self-renewing long-term tumor-propagating cells that resist castration. Cell Stem Cell 2012;10:556-69.
20. Kong, F., Zheng, C. & Xu, D. Telomerase as a "stemness" enzyme. Sci. China Life Sci 2014;57:564-70.
21. Jeter CR, Liu B, Lu Y, et al. NANOG reprograms prostate cancer cells to castration resistance via dynamically repressing and engaging the AR/FOXA1 signaling axis. Cell Discov 2016;2:16041.
22. Jeter CR, Yang T, Wang J, et al. Concise Review: NANOG in Cancer Stem Cells and Tumor Development: An Update and Outstanding Questions. Stem Cells 2015;33:2381-90.
23. Collins AT, Berry PA, Hyde C, et al. Prospective identification of tumorigenic prostate cancer stem cells. Cancer Res 2005;65:10946-51.
24. Li H, Jiang M, Honorio S, et al. Methodologies in assaying prostate cancer stem cells. Methods Mol Biol 2009;568:85-138.
25. Deng Q, Tang DG. Androgen receptor and prostate cancer stem cells: biological mechanisms and clinical implications. Endocr. Relat. Cancer 2015;22:T209-T220.
26. Neumüller RA, Knoblich JA. Dividing cellular asymmetry: Asymmetric cell division and its implications for stem cells and cancer. Genes Dev 2009;23:2675-99.